Proceedings World Geothermal Congress 2015
Melbourne, Australia, 19-25 April 2015

Modeling and Forecasting Induced Seismicity in Deep Geothermal Energy Projects

Eszter Király, J. Douglas Zechar, Valentin Gischig, Dimitrios Karvounis, Lukas Heiniger and Stefan Wiemer

Swiss Seismological Service, ETH Zurich, Sonneggstrasse 5, NO H39.2, CH-8092 Zürich, Switzerland

eszter.kiraly@sed.ethz.ch

Keywords: Basel, CSEP testing, deep geothermal systems, forecasting seismicity, Soultz-sous-Forêts, St. Gallen

ABSTRACT

Over the past decade deep geothermal projects in Switzerland have demonstrated our limited understanding of induced seismicity: unexpected earthquakes occurred during stimulation periods and led to increases in seismic hazard. Such events may influence public opinion of potential future geothermal projects. Monitoring and controlling induced seismicity with warning systems requires models that are updated as new data arrive and that are cast in probabilistic terms (to represent uncertainties in the physical processes and model parameters). Our goal is to improve the forecasting skill owing to validated physical constraints. As a first step, we seek to answer the question: is it possible to reliably forecast the seismic response of the geothermal site during and after stimulation based on observed seismicity and hydraulic data? To answer this question, we are exploring the predictive performance of various stochastic and hybrid models. The aim is to balance model prediction performance and model complexity: which parameters are necessary to forecast seismicity well, and which increase model complexity but do not give better results? The long-term aim of this research is to develop an on-site decision-making tool for geothermal projects to jointly maximize operational safety and economic output during all project phases.

In this preliminary study, we consider four variants of a 3D model that combines seismogenic index calculations with spatial density estimates based on kernel-smoothed seismicity. We apply the model to the Basel 2006-2007, Soultz-sous-Forêts 2004 and St. Gallen 2013 datasets and generate a series of six-hour forecasts. We assess the models using metrics developed by the Collaboratory for the Study of Earthquake Predictability. We check the overall consistency of six-hour forecasts with the observations, comparing the number and spatial distribution of forecast events with the observed induced earthquakes. We also compare models with each other in terms of information gain, allowing a pairwise ranking of the models. Our results indicate that the performance of the model depends on the dataset: the number of forecast events are consistent with the observations in Basel, systematically overestimated for Soultz-sous-Forêts (stimulation of 2004), and underestimated for St. Gallen. Smoothed seismicity models with or without temporal weighting show significantly better results than a model with a spatially uniform distribution in terms of joint log-likelihood, cumulative information gain per earthquake, and average probability gain. In this study, we have not considered the distribution of earthquake magnitudes: each model forecasts only the number of earthquakes above a minimum magnitude.

1. INTRODUCTION

The decision to phase out nuclear power in Switzerland by 2034 has accelerated research on deep geothermal energy, which has the potential to contribute to long-term energy resources. The GEOTHERM project started in 2009 and brought together geoscience, engineering, and social-science groups at ETH Zürich, EPF Lausanne, and the Paul Scherrer Institut with industry representatives from Axpo and GeoEnergy Suisse and public stakeholders from the Bundesamt für Energie. GEOTHERM-2 followed and will continue until April 2016. The project focuses on two problems: (1) the difficulty of engineering a reservoir that is an appropriate heat exchanger within deep, hot, low-porosity rock, and (2) the risk of inducing felt seismic events during the development and long-term usage of the heat exchanger.

Among various types of deep geothermal reservoirs we focus on systems where (1) a sufficient amount of hot water circulates through a highly permeable medium (e.g. Krafla, Iceland, Evans et al., 2012) and (2) the hot rock reservoir has low permeability and small quantity of fluid is present (e.g. Basel, Switzerland, Häring et al., 2008). The former systems are rare, usually found in volcanic regions. On the other hand, the latter are considered to be independent of geological site conditions. When permeability is low, the reservoir needs to be created (i.e., permeability has to be enhanced) so that fluid can circulate in a closed loop (Majer et al., 2007). Permeability enhancement in these engineered reservoirs (Enhanced Geothermal Systems, EGS) is usually done with high pressure stimulations using water or acidic fluid. The process of enhancing permeability is associated with seismic events that are usually micro-earthquakes ($m_w < 3.0$), but larger events can occur such as magnitude 4 – 5 (Majer et al., 2007). Felt earthquakes raises public concerns about geothermal projects.

The key element of reservoir design schemes avoiding large induced earthquakes is the ability plan based on potentially foreseen seismic events. However, it is clear that precise prediction of events is difficult to achieve before stimulations. It is not easy even during stimulations since we do not fully understand the governing mechanisms of induced seismicity and its precise subsurface properties. Shapiro et al., (2010) proposed a site-specific parameter, called seismogenic index, which represents the potential seismic response of the given site. It can be calculated from a short injection period as well as from the whole stimulation taking into account the b-value of the observed seismicity and total injected volume. This allows a relative comparison between the seismic response of geothermal sites pointing out high seismic activities compared to total injected volume with high value of seismogenic index. However, seismogenic index does not yield information on the spatio-temporal variation of induced seismicity.

In our group a multidisciplinary project has been started to develop an Advanced Traffic Light and Assessment System for induced seismic hazard analysis (e.g., Bachmann et al., 2011; Goertz-Allmann and Wiemer, 2013; Mena et al., 2013). Several models have been developed to date, some statistical (e.g., Reasenberg and Jones, 1989; Hainzl and Ogata, 2005; Bachmann et al., 2011; Mena

et al., 2013) and some physics-based numerical models (e.g., Bruel, 2005; Kohl and Mégel, 2007; Baisch et al., 2010; Rutqvist, 2011; McClure and Horne, 2012; Wang and Ghassemi, 2012; Karvounis, 2013). Statistical models are simple, quick and give realistic seismicity forecast for the period when data are available (Mena et al., 2013). However, they do not model permeability creation, do not account for the governing physical processes and they cannot give good constrains for longer time periods i.e., several weeks, month, years after the stimulation. Moreover, they are not able to capture unexpected events (e.g., large magnitudes). Thus, they have limited capabilities for investigation of long-term intervals, post-injection behavior or alternative injection scenarios.

The main advantage of physics-based models is that they reasonably represent the underlying physical processes. Hence, they have the capability to improve the forecast for longer periods, to predict unexpected events, and to study phenomena with sensitivity analyses. However, they do not necessarily account for epistemic uncertainties (i.e., uncertainty due to the lack of knowledge or data) and intrinsic randomness of seismicity. Moreover, due to their computational expenses they cannot be applied in near-real time. Thus, no comprehensive physics-based model exists to date that can be used in an induced seismic hazard assessment framework.

An attempt to exploit advantages of statistical models (efficiency) and physics-based models (physical process representation) are so-called hybrid models as described by Goertz-Allmann and Wiemer (2013). They developed a geomechanical forward model where rupture initiation occurs due to simple, homogeneous, isotropic pore pressure diffusion on randomly placed potential earthquake nucleation points (seeds). Gischig and Wiemer (2013) expanded this model to include the wellhead pressure as an additional constraint; in their model earthquakes are triggered by a pressure field that is based on non-linear pressure diffusion with irreversible permeability enhancement.

Having models with different complexity levels, we seek to answer the question: is a certain degree of model complexity necessary to forecast micro-seismicity and unexpected, large events well, or does it only increase model complexity without giving better results? To answer this question, a model development and "test bench" is being built up following the guidelines of the Collaboratory for the Study of Earthquake Predictability (CSEP, http://www.cseptesting.org/centers/eth). CSEP operates testing centers providing support for scientific prediction experiments in multiple regional or global natural laboratories. Successful testing has been performed for Italy and Southern California. Testing is carried out with well-established statistical tools in a controlled environment: at first, model consistency with respect to the observed data is examined, then pairwise comparisons of models are performed. Similar systematic testing of induced seismicity models has the potential to balance model prediction performance and model complexity.

In this context, we think of forecasting in terms of two time intervals: a learning and a forecast period. During the learning period the model "learns" about the actual dataset, then gives an estimation of the particular process for the (near) future, the forecast period. In the context of seismicity, during the learning period a certain number of seismic events are observed, analyzed according to their distribution in time and space. Then a calibrated model forecasts the number and spatial distribution of events for a given time interval in the future. Classical seismic forecasts give the location of the earthquakes in latitude-longitude position, the order of magnitude of forecast time period is years. However, for induced seismic events in geothermal systems, the vertical component of an event location plays an important role, thus 3D position of the events is needed. Additionally, the forecast period must be at the order of hours or days for short-term, weeks or months for long-term forecasts.

In this paper, we present a model based on the seismogenic index (Shapiro et al., 2010) and a simple seismicity decay (Langenbruch and Shapiro, 2010) with 4 different spatial kernels. The aim is to show how this model performs with respect to three different datasets (Soultz-sous-Forêts 2004, Basel 2006-2007 and St. Gallen 2013) and if we can give a reasonable hint on spatial forecasting in the next 6 hours following learning periods. Additional datasets from all over the world, such as Cooper Basin (Australia), Ogachi, Hijori (Japan) (Kaieda et al., 2010), Berlín (El Salvador) (Bommer et al., 2006) are potential targets of further work if datasets are available, they are sufficiently complete and data quality is appropriate.

2. DATASETS

The Soultz-sous-Forêts geothermal site is located near Soultz-sous-Forêts in the roughly N-S striking normal faulting Rhine Graben (Zoback, 1992), about 70 km north of Strasbourg in Alsace (France). The geothermal gradient is about 100 °C/km within the 1.5 km thick sedimentary cover over a granitic basement (Evans et al., 2012). The geothermal project started in the early 1980s. Over the following 30 years, 4 wells were drilled into 2 reservoirs: a shallow reservoir at about 3.5 km depth (GPK1, GPK2 wells), and a deep reservoir at about 4.5 km (GPK2, GPK3, GPK4 wells). Several stimulations and circulation tests were carried out. Energy production started in 2008. In this work we used the stimulation dataset of September 2004.

The Basel geothermal site is located at the south-eastern margin of the Upper Rhine Graben similarly to Soultz-sous-Forêts, on the Swiss portion of the graben. The granitic basement is covered by 2.4 km sedimentary rocks. The well was drilled to 5 km depth in October 2006. After several tests, the reservoir was hydraulically stimulated to enhance its permeability in December 2006. After 6 days the injection was stopped due to intensive seismicity including events with magnitudes reaching mL = 2.6. Five hours after the well was stopped, a mL = 3.4 event occurred, followed by additional shocks of mL>3.0 (Häring et al., 2008). Based on the results of a subsequent risk study, it was decided to abandon the project.

The St. Gallen geothermal site is located in north-eastern Switzerland, about 5 km west of the city of St. Gallen. The stress regime includes local extension observed along strike-slip faults. According to Singer et al., (2014) the stress field is the local expression of the active convergence of the European and Adriatic plate north of the Alpine front. A 3D seismic campaign revealed a fault at 4-5 km depth in the Malm formation below the 4 km-thick molasse. This fault was targeted to use pre-existing high permeability. The temperature at that depth is ~200 °C (Geowatt AG et al., 2009). Drilling operations started in March 2013 and an injection test was carried out on 14 July. Then, to enhance the connection between the well and the formation, acid-working fluid was pumped into the well on 17 July, this was accompanied by a low seismicity rate. On 19 July gas flow was observed in the well, and the gas flow resulted in increasing well-head pressure. To control the well, heavy mud was injected, and this in turn increased seismic activity.

Due to the injection of about 700 m³ working fluid about 700 earthquakes were recorded including a shock of mw = 3.3 (20 July, 3:30am). The event was followed by a rapid decrease of well-head pressure, steady mud loss, and gas entry (Kraft et al., 2013). About 300 events were later relocated with the double difference method, and the resulting relocations highlight a clear lateral structure in the Mezozoic sediments below the openhole (Diehl et al., 2013). A production test was carried out in November 2013, during which very few earthquakes occurred. Stakeholders called for a risk study: a decision on the project future will be made in September 2014 (Kraft et al., 2013).

Injection strategies and seismicity clouds of these datasets show very different characteristics. The stimulation in Soultz 2004 produced a huge number of earthquakes with only moderate magnitudes. In the case of Basel 2006, a moderate number of events was induced but larger earthquakes (mw > 2.5) occurred some hours and days after the injection had stopped, and the activity continued in the following weeks and months. The injection in St. Gallen 2013 induced hundreds of events but the largest event (mw = 3.3) occurred after 1 day of injection.

3. MODEL SETUP

Our aim is to forecast the number and spatial distribution of seismic events in the next 6 hours. The model consists of two parts: firstly, we determine the amount of seismic events for the forecast period, secondly, we determine their spatial distribution in the reservoir. Ideally seismicity should be determined before the fluid injection starts, however, this is extremely difficult. We need to calibrate our model for a learning period to give reasonable forecast. In this study, we use a learning period that starts as the fluid injection starts, and grows gradually with 6-hour steps. Similarly to Mena et al., (2013), forecast periods are additional 6-hour periods following the learning periods. Maximum lengths of the learning periods depend on the available data, so it is different for the three datasets. In case the of Basel, we started to forecast after 1 day of learning period, then we expanded it to 12 days, then to 62 days. In the case of St. Gallen and Soultz 2004, the shortest learning period was 0.7 day and it finally reached the length of 10 days. In the following subsections we explain how the number of events and their spatial distribution are forecast.

3.1 How Many Earthquakes Will Occur?

To determine the number of forecast events, we use two sub-models: one based on the seismogenic index (Shapiro et al., 2010) and used during stimulation and one used after stimulation based on the decay of seismicity with time (Langenbruch and Shapiro, 2010).

The number of earthquakes during stimulation is forecast by the following equation:

$$\log\big(N_m(t)\big) = \log\big(Q_c(t)\big) - \mathrm{bm} - \Sigma\,, \tag{1}$$

where $N_m(t)$ indicates the total number of induced events above magnitude m up until time t, Q_c, denotes the cumulative injected volume of fluid at time t, b is Gutenberg-Richter b-value of the observed seismicity, m is the magnitude cut-off (here it is the magnitude of completeness), and $\sum$ is the seismogenic index. A comparison of deep geothermal datasets (Király et al., 2014) showed that b and $\sum$ are not constant during and after stimulation. Thus we re-estimate them at the end of each learning period. Q_c is estimated by extrapolating the trend of the last 6 hours of the cumulative injected fluid volume. We use equation (1) to estimate the total number of induced earthquakes at the end of the forecast period, thus we need to subtract the number of observed events to calculate the seismicity rate for the forecast period.

As soon as the stimulation stops, we use a post-stimulation forecast model based on a simple seismicity decay (Langenbruch and Shapiro, 2010). The number of earthquakes after stimulation is described by the following equation:

$$R_{0\mathrm{b}}\left(\frac{t}{t_0}\right) = \frac{R_{0\mathrm{a}}}{\left(\frac{t}{t_0}\right)^p}\,, \tag{2}$$

where R_{0b} is post-stimulation seismicity rate at time t, t_0 indicates the moment when stimulation stops, R_{0a} denotes constant seismicity rate during stimulation, and p describes the rate decay. As in CSEP experiments and suggested by Shapiro et al., (2010), the number of events in each forecast is assumed to follow a Poisson distribution and the numbers obtained by using Equations (1) and (2) are Poisson expected values.

3.2 Where Will Events Occur?

One might consider that observed induced seismic events of hydraulic stimulations can provide useful information about the spatial distribution of future induced earthquakes. Several studies, including the Regional Earthquake Likelihood Models (RELM) experiment (Field, 2007; Zechar et al., 2010) showed that smoothed seismicity models are effective at forecasting earthquake locations in natural seismicity. These models typically use nonparametric kernel smoothing and place two-dimensional Gaussian kernels on each past seismic event (e.g. Helmstetter et al., 2007). Individual contributions of observed earthquakes are summed and normalized to create an overall probability density function (earthquake density map) in a given grid. In the context of induced seismicity one has to pay attention to the depth of events since shaking intensity at the surface depends not only on the magnitude of an event but also on its depth. Due to the fact that geothermal reservoirs can be quite close to settlements, one can benefit if event locations are forecast in 3D. Thus, we use a 3D Gaussian smoothing kernel with a fixed 100 m bandwidth dimensions to create a probability density function in the whole reservoir. The probability density function is updated as the length of the learning period increases. This approach assumes that earthquake locations in the 6 hour forecast period will not be very different from the seismicity observed so far.

One of the challenges that is absent in the case of tectonic earthquakes is to be able to reproduce the Kaiser effect (i.e., decrease of seismic activity in the vicinity of the injection well after the pump has stopped) since the majority of the earthquakes occur in the vicinity of the well. To address this, we apply a temporal weighting that gives more emphasis to recent events than older ones. Two types of weighting are considered here: Heaviside and exponential (figure 1). In the case of Heaviside weight, we give maximum

weight (one) to those earthquakes that occurred in the last 1 or 2 days (it depends on the dataset and the length of the tested period), and previous events are ignored (they get zero weight). This corresponds to a moving window approach, rather than a growing window (see also Zechar and Nadeau, 2012). In the case of exponential weight, events are weighted according to a simple exponential function with time: maximum weight (one) is attributed to the event that occurred at the end of the learning period, earlier events get smaller weights according to their occurrence time. This is analogous to the exponential smoothing approach commonly used in time series forecasting (Goodwin, 2010) and is also connected to the Omori-Utsu relation describing aftershock decay rate (Zhuang et al., 2012).

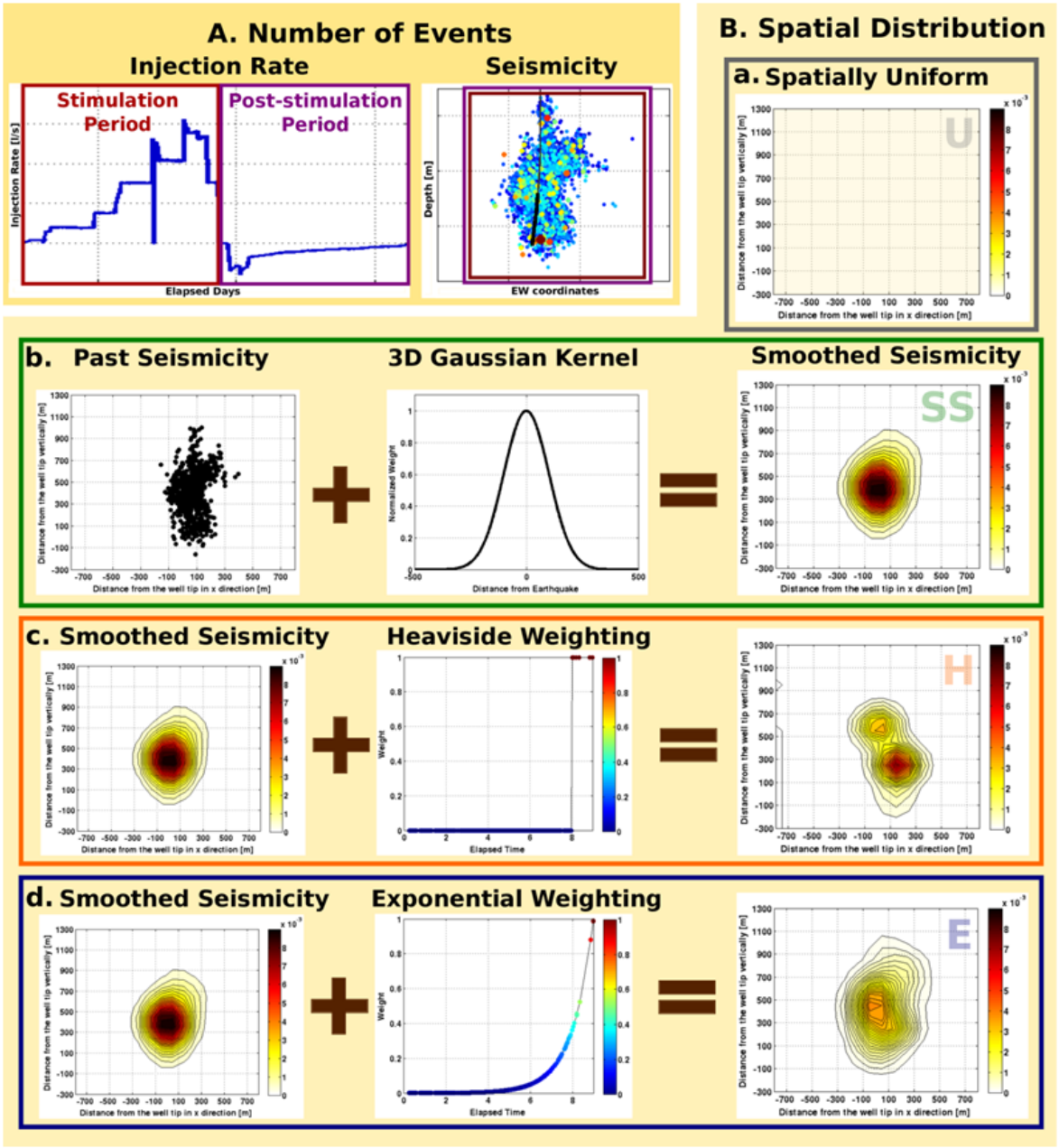

Figure 1. A. Explanation how to calculate the number of forecast earthquakes. See also Equation (1) and (2). B. Spatial distribution of forecast events: a. uniform distribution (gray frame), b. smoothed seismicity (green frame), c. smoothed seismicity with 1 or 2 days long moving window (orange frame) and d. smoothed seismicity with exponential temporal weight (blue frame). Panels of the right column show vertical cross sections of the corresponding 3D probability density functions. Basel 2006 dataset is used for illustrations.

In the following sections we present the forecast testing of 4 models based on Shapiro's number estimation (figure 1.A) and different spatial kernels (figure 1.B):

- Spatially uniform distribution model: assumes that induced earthquakes are equally likely everywhere in the study region (figure 1.B.a. gray frame), i.e., the seismicity rate is homogeneous in the whole reservoir.

- Smoothed seismicity model: uses observed seismicity to create a probability density function of the reservoir applying 3D Gaussian kernels on each event (figure 1.B.b. green frame).

- Smoothed seismicity with Heaviside weighting uses smoothed seismicity model applying a 1 or 2 day moving window to highlight more recent induced earthquakes (figure 1.B.c. orange frame). Length of the moving window is 1 day in the case of Soultz 2004 and Basel 2006 datasets (12 days time window), 2 days for St. Gallen 2013 dataset. This model is not applied in the case of Basel 2006-2007 dataset (62 days time window) due to the rare occurrence of induced events.

- Smoothed seismicity with exponential weighting uses smoothed seismicity model applying a simple temporal exponential function to highlight more recently induced earthquakes (figure 1.B.d. blue frame).

4. FORECAST TESTS

We apply forecast tests using the guidelines of the CSEP testing center in a pseudo-prospective way, which means that data that we test against are already available. First, we check if the model is consistent with the data. Thus, we test if the overall number of earthquakes in all forecast periods is consistent with the observed number of events of the corresponding time window (Number-test). To test the spatial component as well (Space-test), i.e., if the spatial distribution of forecast and observed events are in good agreement (Zechar, 2010; Rhoades et al., 2011), we consider a 4 x 4 x 4 km reservoir around the well tip or the center of the seismicity cloud. The reservoir is divided into 100 x 100 x 100 m voxels. After normalizing the forecasts so that the total number of forecast events matches the total number of observed events, we calculate the logarithm of the Poisson distribution given the number of observed earthquakes and the seismicity forecast rate in each voxel. Summing up these values gives a joint log-likelihood (LL hereafter) of a specific experiment (a 6-hour forecast period). To define if the forecast is good enough, we simulate 1000 of LL given the forecast and find the 5% of the simulated joint LL. If the joint LL corresponding to the actual observation is higher than the 5%, the forecast passed the null-hypothesis test – the observed seismicity could have been generated by the model. We compute joint LL of each experiment and an overall joint LL value, which is characteristic for the model performance of the whole testing period. The higher the joint LL values are the better the model (Zechar, 2010; Rhoades et al., 2011).

In order to compare the models, the Student's paired t-test (Student, 1908) is used. We calculate the information gain of a sample of population with a correction concerning the number of events of the samples. Here we investigate if smoothed seismicity models give better forecast than a spatially uniform distribution, which means that we compare the forecast seismicity rates of a smoothed seismicity model with the spatially uniform distribution rates. The following formula gives the information gain per earthquake to a sample of population (Rhoades et al., 2011).

$$I_N = \frac{1}{N} \sum_{i=1}^{N} \ln\left(\frac{\lambda_{A_i}}{\lambda_{B_i}}\right) - \frac{N_A - N_B}{N} \ , \tag{3}$$

where I_N indicates information gain per earthquake of a sample of population, N is the number of observed events of the sample, λ_{Ai} *and* λ_{Bi} denote forecast seismicity rate in the ith voxel of model A and B, respectively, N_A and N_B are number of events of the sample in model A and B, respectively. Exponentiating the information gain per earthquake yields the average probability gain of model A with respect to model B.

5. RESULTS AND DISCUSSION

With some exceptions, the Shapiro model produces forecasts that are consistent with the number of seismic events in 6h intervals during the Basel stimulation (figure 2.). Yet, it does not forecast the seismic swarms that appear in the weeks and months after the stimulation. For the Soultz 2004 stimulation, the model systematically overestimates the number of events except the first 7-8 experiments; and, it severely underestimates in St. Gallen 2013 (with some insignificant exceptions). This difference in model performance could result from the variation of the seismic and hydraulic properties of the different geothermal projects.

Regarding the spatial component of the model, we find that (figure 3):

• In general smoothed seismicity models perform quite similarly, and the spatially uniform model differs remarkably from the smoothed seismicity models.

• Joint LL evolution of the smoothed seismicity models show better forecasting skills during stimulations and approximately 4 days following the shut-in than the spatially uniform model.

• Approximately 4 days after the stimulations, smoothed seismicity models do not perform significantly better than the spatially uniform model in terms of joint LL. This observation can be due to the fact that only a few events occurred at the end of the testing time window.

• In terms of joint LL for all experiments (values on the panels of figure 3), smoothed seismicity models perform better than the spatially uniform model.

These findings indicate that smoothed seismicity models give significantly better seismicity rate forecast than the spatially uniform model during and shortly after the injection period. Comparison of individual smoothed seismicity models with respect to the spatially uniform model also supports this finding (figure 4). The Soultz 2004 dataset gives the smallest information gain per earthquake at the end of the investigated time period (5.7-5.9, figure 4.B) with respect to the spatially uniform model; the Basel 2006-2007 project yields intermediate values (5.9-6.3, figure 4.A) and the highest values are from the St. Gallen 2013 dataset (7.4-7.6, figure 4.C). These values can be translated to average probability gain of 365, 544.5 and 1998.2 for Soultz 2004, Basel 2006-2007 and St. Gallen 2013, respectively, meaning that, for example, in St. Gallen in the voxels where earthquakes occurred, the smoothed seismicity forecasts have a rate that is on average 1998.2 times that of the spatially uniform model. Comparison of the 3 smoothed seismicity models shows that on average they perform equally well in the S-test and with respect to the spatially uniform model. Exponentially-weighted smoothed seismicity model performs slightly better than the others with respect to the spatially uniform model in all tested datasets.

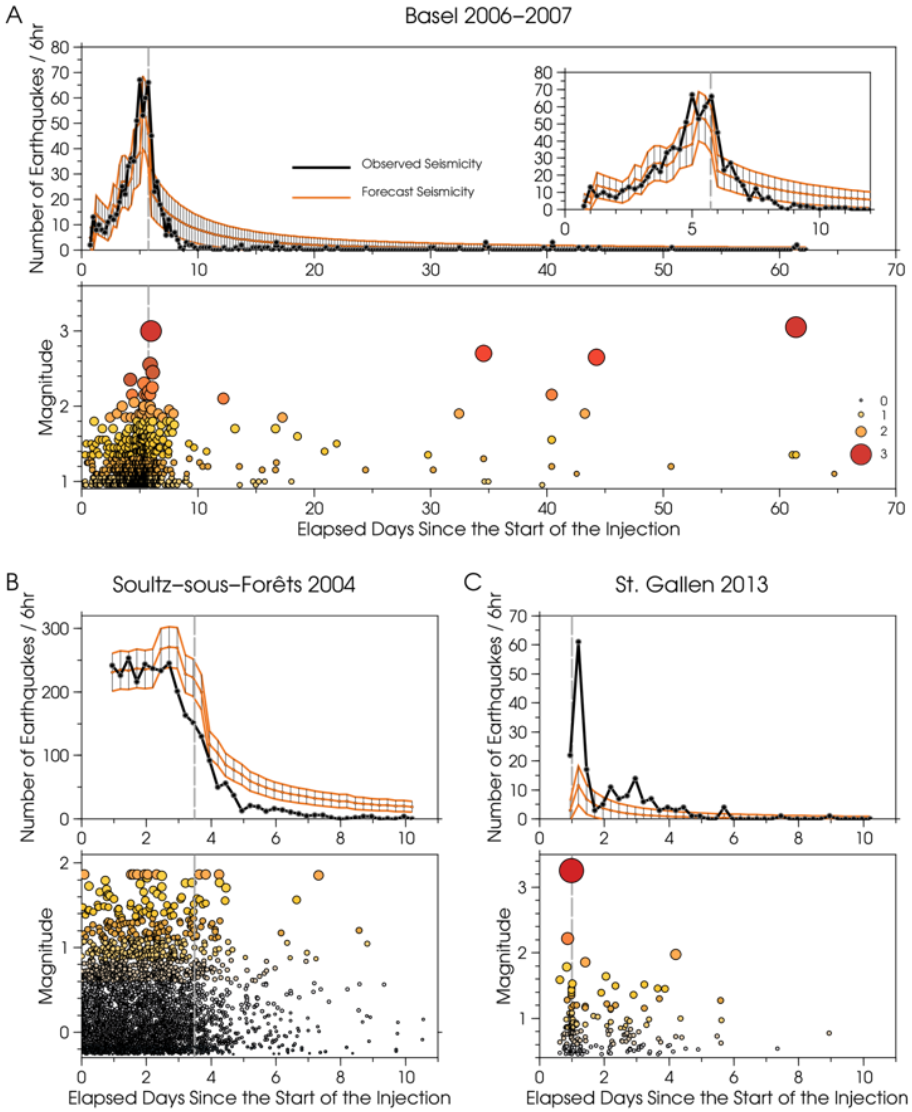

Figure 2. A, B and C parts of the figure show Basel 2006-2007, Soultz-sous-Forêts 2004 and St. Gallen 2013 datasets, respectively. The inset of part A is a zoom of the Basel dataset between 2 - 14 Dec. Upper panels: comparison of the number of forecast (red dots) and observed events (black dots) in function of time. Error bars are calculated from the 95% confidence interval of the Poisson distribution. Gray dashed line indicates the time when the pumps were stopped. Lower panels: magnitudes of induced earthquakes in function of time, colors correspond to magnitudes. Gray dashed line indicates the time when the pumps were stopped.

6. CONCLUSION

In this study we consider the predictive performance of induced seismicity models using metrics developed by the Collaboratory for the Study of Earthquake Predictability. We check the consistency of each model with observed seismicity and compare models with each other.

We find that the performance of the Shapiro model depends on the dataset: in the case of Basel 2006-2007 project, it generally produces forecasts consistent with the observations; in the case of Soultz-sous-Forêts 2004 project, it overestimates the number of earthquakes; for the St. Gallen 2013 dataset, it systematically underestimates the number of earthquakes. Moreover, the model does not represent well seismicity in the long-term and even post-injection seismicity. However, instability of the model performance could be due to the variation of seismic and hydraulic properties of the tested datasets.

Concerning the spatial component of the model, smoothed seismicity models (with or without temporal weighting) generally show significant skill – in terms of joint log-likelihood, cumulative information gain per earthquake and average probability gain – relative to a model with a spatially uniform distribution. The spatial improvement is most noticeable in the St. Gallen 2013 dataset, possibly due to the particular shape of the seismicity, which is not well-described by a spatially uniform model.

Comparison of the three smoothed seismicity models shows that on average they perform equally well in a spatial consistency test, and they all have roughly equal predictive skill when compared to the spatially uniform model. In all experiments, the smoothed seismicity model with exponential temporal weighting performs slightly better than the others with respect to the spatially uniform model.

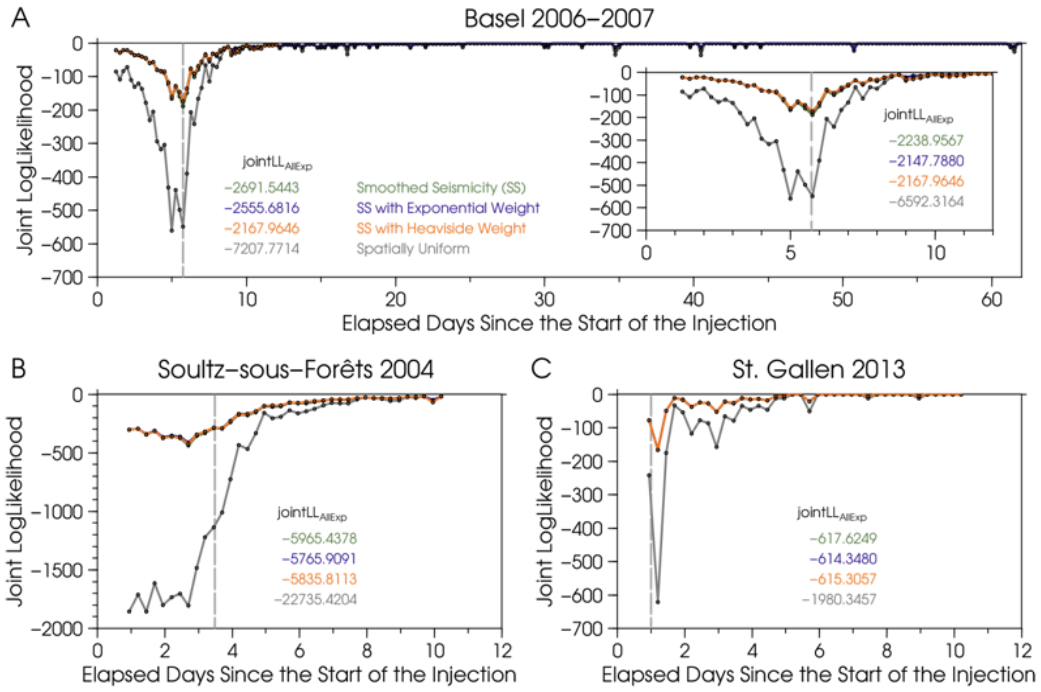

Figure 3. Evolution of joint log-likelihood values for each experiment in function of time. A, B and C parts of the figure show Basel 2006-2007, Soultz-sous-Forêts 2004 and St. Gallen 2013 datasets, respectively. The inset of part A is a zoom of the Basel dataset between 2 - 14 Dec. Gray, green, orange and blue lines indicate the spatially uniform, smoothed seismicity, smoothed seismicity with moving window and smoothed seismicity with exponential temporal weight, respectively. Values on the panels give the joint log-likelihood value for all experiments with the corresponding colors. The length of the moving window is 2 days for St. Gallen 2013, 1 day for Soultz-sous-Forêts 2004 and Basel 2006 datasets. Due to the lack of induced earthquakes this approach is not applied for the Basel 2006-2007 experiment. Gray dashed line indicates the time when the pumps were stopped.

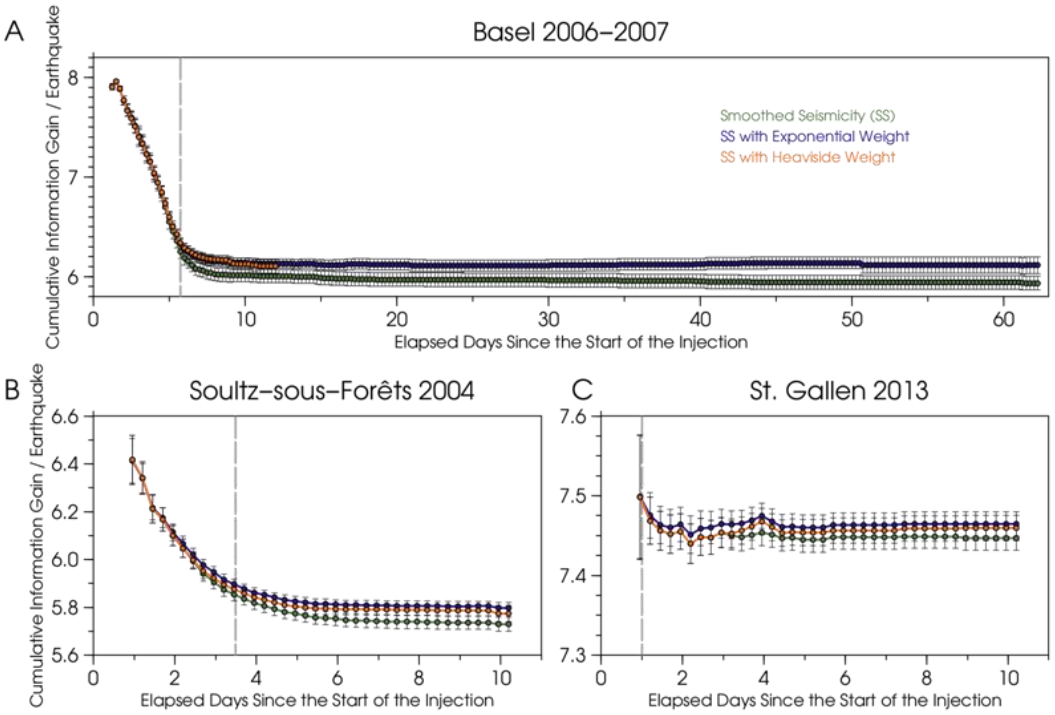

Figure 4. Evolution of cumulative information gain per earthquake with respect to the uniform distribution. A, B and C parts of the figure show Basel 2006-2007, Soultz-sous-Forêts 2004 and St. Gallen 2013 datasets, respectively. Green, orange and blue colors correspond to smoothed seismicity, smoothed seismicity with moving window and smoothed seismicity with exponential temporal weight, respectively. The length of the moving window is 2 days for St. Gallen 2013, 1 day for Soultz-sous-Forêts 2004 and Basel 2006 datasets. Due to the lack of induced earthquakes this approach is not applied for the Basel 2006-2007 experiment. Gray dashed line indicates the time when the pumps were stopped.

These preliminary findings suggest that real-time analysis of seismic data and kernel smoothing can improve spatial forecasts of seismicity, and thus, can provide useful information for real-time reservoir planning and risk assessments. In future work, we intend to include tests of magnitude distribution, and will consider additional models such as that of Gischig and Wiemer (2013). Comparison of fundamentally different models can give a hint as to which parameters are essential to improve model prediction performance of micro-seismicity and large, unexpected earthquakes for short and long periods.

7. ACKNOWLEDGMENT

We acknowledge the GEOTHERM-2 project (http://www.cces.ethz.ch/projects/nature/geotherm-2) for funding this PhD project. We thank the St. Galler Stadtwerke (SGSW) and Toni Kraft for providing the data of the St. Gallen geothermal project, and Tobias Diehl for the relocated event coordinates. We also thank an anonymous reviewer for his/her suggestions that helped to improve the paper.

REFERENCES

Bachmann, C. E., Wiemer, S., Woessner, J., and Hainzl, S.: Statistical analysis of the induced Basel 2006 earthquake sequence: introducing a probability-based monitoring approach for Enhanced Geothermal Systems, Geophys. J. Int., 186, (2011), 793–807.

Baisch, S., Vörös, R., Rothert, E., Stang, H., Jung, R., and Schellschmidt, R.: A numerical model for fluid injection induced seismicity at Soultz-sous-Forêts, Int. J. Rock Mech. Min. Sci., 47, (2010), 405–413.

Bommer, J. J., Oates, S., Cepeda, J. M., Lindholm, C., Bird, J., Torres, R., Marroquín, G., and Rivas, J.: Control of hazard due to seismicity induced by a hot fractured rock geothermal project, Engineering Geology, 83, (2006), 287-306.

Bruel, D.: Using the Migration of Induced Micro-Seismicity as a Constraint for HDR Reservoir Modelling, Proceedings, Thirtieth Workshop on Geothermal Reservoir Engineering, Stanford University, Stanford, CA (2005).

Diehl, T., Kraft, T., Kissling, E., Deichmann, N., Wiemer, S., Clinton, J., Haslinger, F., and Waldhauser, F.: Near-real-time high-precision relocation of induced seismicity in the geothermal system below Sankt Gallen (Switzerland), Proceedings, AGU 2013.

Evans, K. F., Zappone, A., Kraft, T., Deichmann, N., and Moia, F.: A survey of the induced seismic responses to fluid injection in geothermal and CO2 reservoirs in Europe, Geothermics, 41, (2012), 30–54.

Field, E. H.: Overview of the Working Group for the Development of Regional Earthquake Likelihood Models (RELM), Seismol. Res. Lett., 78, (2007).

Geowatt AG, Z., S. G. Support, Foralith Drilling AG, F. Dr. Roland Wyss GmbH, S. G. Dr. Heinrich Naef - Büro für angewandte Geologie & Kartografie, and W. Progeo GmbH: Machbarkeitsstudie Tiefengeothermie Stadt St . Gallen Konzept für die Entwicklung (Planung und Erstellung) einer Geothermieanlage in der Stadt St. Gallen, (2009).

Gischig, V. S., and Wiemer, S.: A stochastic model for induced seismicity based on non-linear pressure diffusion and irreversible permeability enhancement, Geophys. J. Int., 194, (2013), 1229 – 1249.

Goertz-Allmann, B. P., and Wiemer, S.: Geomechanical modeling of induced seismicity source parameters and implications for seismic hazard assessment, Geophysics, 78, (2013), KS25–KS39.

Goodwin, P.: The Holt-Winters approach to exponential smoothing: 50 years old and going strong. Foresight, 19, (2010) 30-34.

Hainzl, S., and Y. Ogata: Detecting fluid signals in seismicity data through statistical earthquake modeling, J. Geophys. Res., 110, (2005), B05S07.

Häring, M. O., Schanz, U., Ladner, F., and Dyer, B. C.: Characterisation of the Basel 1 enhanced geothermal system, Geothermics, 37, (2008), 469–495.

Helmstetter, A., Kagan, Y. Y., and Jackson, D. D.: High-resolution Time-independent Grid-based Forecast for M >= 5 Earthquakes in California, Seismol. Res. Lett., 78, (2007), 78–86.

Kaieda, H., Sasaki, S., and Wyborn, D.:Comparison of Characteristics of Micro-Earthquakes Observed During Hydraulic Stimulation Operations in Ogachi, Hijiori and Cooper Basin HDR Projects. Proceedings, World Geothermal Congress 2010, (2010).

Karvounis, D. C.: Simulations of Enhanced Geothermal Systems with an Adaptive Hierarchical Fracture Representation. PhD Thesis (2013).

Király, E., Gischig, V., Karvounis, D., and Wiemer, S.: Validating Models to Forecasting Induced Seismicity Related to Deep Geothermal Energy Projects, Proceedings, 39th Workshop on Geothermal Reservoir Engineering, Stanford University, Stanford, CA (2014).

Kohl, T., and Mégel, T.: Predictive modeling of reservoir response to hydraulic stimulations at the European EGS site Soultz-sous-Forêts, Int. J. Rock Mech. Min. Sci., 44, (2007), 1118–1131.

Kraft, T., Wiemer, S., Deichmann, N., Diehl, T., Edwards, B., Guilhem, A., Haslinger, F., Kiraly, E., Kissling, E., Mignan, A., Plenkers, K., Roten, D., Seif, S., and Woessner, J.: The ML3.5 induced earthquake sequence at Sankt Gallen, Switzerland., Proceedings, AGU 2013.

Langenbruch, C., and Shapiro, S. A.: Decay rate of fluid-induced seismicity after termination of reservoir stimulations, Geophysics, 75, (2010), 1–10.

Majer, E., Baria, R.,Stark, M., Oates, S., Bommer, J., Smith, B., and Asanuma, H.: Induced seismicity associated with Enhanced Geothermal Systems, Geothermics, 36, (2007), 185-222.

McClure, M. W., and Horne, R. N.: Investigation of injection-induced seismicity using a coupled fluid flow and rate / state friction model, Geophysics, 76, (2012), WC181 – WC198.

Mena, B., Wiemer, S., and Bachmann, C.: Building Robust Models to Forecast the Induced Seismicity Related to Geothermal Reservoir Enhancement, Bull. Seismol. Soc. Am., 103, (2013), 383–393.

Reasenberg, P. A., and Jones L. M.: Earthquake Hazard After a Mainshock in California, Science, 243, (1989), 1173 – 1176.

Rhoades, D. A., Schorlemmer, D., Gerstenberger, M. C., Christophersen, A., Zechar, J. D., and Imoto, M.: Efficient testing of earthquake forecasting models, Acta Geophys., 59, (2011), 728–747.

Rutqvist, J.: Status of the TOUGH-FLAC simulator and recent applications related to coupled fluid flow and crustal deformations, Comput. Geosci., 37, (2011), 739–750.

Shapiro, S. A., Dinske, C., Langenbruch, C., and Wenzel, F.: Seismogenic index and magnitude probability of earthquakes induced during reservoir fluid stimulations, LeadingEdge - Spec. Sect. Microseismic, (2010), 304–309.

Singer, J., Diehl, T., Husen, S., Kissling, E., and Duretz, T.: Alpine lithosphere slab rollback causing lower crustal seismicity in northern foreland, Earth Planet. Sci. Lett., 397, (2014), 42–56.

Student: The Probable Error of a Mean, Biometrika, 6, (1908), 1 – 25.

Wang, X., and Ghassemi, A.: A 3D Thermal-Poroelastic Model for Geothermal Reservoir Stimulation, Proceedings, 37th workshop on Geothermal Reservoir Engineering, (2012).

Zechar, J. D.: Evaluating earthquake predictions and earthquake forecasts : a guide for students and new researchers, Community Online Resource for Statistical Seismicity Analysis, (2010), doi:10.5078/corssa-77337879.

Zechar, J. D., Gerstenberger, M. C., and Rhoades, D. A.: Likelihood-Based Tests for Evaluating Space-Rate-Magnitude Earthquake Forecasts. Bulletin of the Seismological Society of America, 100, (2010), 1184–1195.

Zechar, J. D., and Nadeau, R. M.: Predictability of repeating earthquakes near Parkfield, California, Geophysical Journal International, 190 (2012), 457-462.

Zhuang, J., Harte, D., Werner, M. J., Hainzl, S., and Zhou, S.: Basic models of seismicity: temporal models, Community Online Resource for Statistical Seismicity Analysis., (2012), doi:10.5078/corssa-79905851.

Zoback, M. L.: First- and second-order patterns of stress in the lithosphere: The World Stress Map Project, J. Geophys. Res., 97, (1992), 11703.